**Supplementary material**
**Balco, G., Rovey, C.W., II., 'Early and middle Pleistocene Laurentide Ice Sheets'**

---

*Materials and Methods.*

*Analytical methods.* We disaggregated paleosol samples in water and isolated the 0.25-0.85 mm grain size fraction by wet-sieving, then extracted and purified quartz using heavy-liquid separation and repeated etching in HF *(S1)*. This yielded quartz samples with 20-100 ppm Al.

We extracted Be and Al from quartz by HF dissolution followed by ion exchange chromatography *(S1)*, then measured Be and Al isotope ratios by accelerator mass spectrometry at the Lawrence Livermore National Laboratory, Center for Accelerator Mass Spectrometry (LLNL-CAMS). We measured total Al in the samples by extracting aliquots from the dissolved quartz-HF solution, evaporating HF in the presence of $H_2SO_4$, redissolving in dilute $HNO_3/H_2SO_4$, and measuring Al concentrations by ICP optical emission spectrophotometry against gravimetrically prepared Al standards. Each total Al determination reflects at least two duplicate analyses on each of at least two separate aliquots.

Al isotope ratios were normalized to the 'KNSTD' standard series *(S2)*. Be isotope ratios were normalized at the time of measurement to a variety of Be standards; for this work we have renormalized all Be measurements to the '07KNSTD' isotope ratio standards of *(S3)*.

Total process blanks contained 65000 $\pm$ 40000 atoms $^{26}$Al, 0.2-1.3 % of the total number of atoms in any sample. We used two different $^{9}$Be carriers. For high-nuclide-concentration samples, we used a commercially available Be standard solution. Total process and carrier blanks using this carrier had 175000 $\pm$ 20000 atoms $^{10}$Be, 0.7-2% of the total number of atoms in any sample. For low-concentration samples, we used several Be carrier solutions derived from deep-mined beryl. Total process and carrier blanks using these carrier solutions had 3000-20000 atoms $^{10}$Be, 0.1-1.3% of the total number of atoms present in any sample.

Table S1 lists $^{26}$Al and $^{10}$Be concentrations.

*Data reduction and age determinations.* Calculations of both simple burial ages and isochron burial ages use implicit solution methods to account for post-burial nuclide production by deeply penetrating muons. Basically, one i) begins by computing an apparent burial age assuming burial at infinite depth, ii) calculates the post-burial nuclide production at the actual sample depth given that burial age, iii) subtracts this nuclide inventory from the measured nuclide inventory, iv) recalculates the burial age, and v) iterates steps i-iv until the calculation converges on a solution. Alternatively, this can be described as an optimization problem in which one finds the burial age that best fits a forward model for nuclide accumulation and decay that includes a burial history inferred from the site stratigraphy and any other relevant geologic evidence.

The methods for computing simple burial ages and isochron burial ages are described in detail in *(S4)* and *(S5)*, respectively. *(S5)* includes MATLAB code for computing isochron burial ages; however, this study used a different Be isotope ratio standardization and $^{10}$Be decay constant, so a variety of constants in this code must be updated to yield the burial ages we report in the present

work. Both simple and isochron burial dating methods use a 'sawtooth' age/depth model in which successive layers of overburden are instantaneously emplaced and then experience steady erosion until emplacement of the next unit, as described in *(S4)*. Thus, calculating a burial age from any of our sites requires: i) the number, thickness, and density of all overburden units, ii) an estimate for age of overburden units that overlie the unit to be dated, and iii) an estimate for the surface erosion rate that prevails between the emplacment of one overburden unit and the next. Thicknesses and densities of overburden units are tabulated in Table S2; our methods for density measurement are described in *(S1)*. To obtain age estimates for overburden units above the one being dated, we began by calculating the ages of the uppermost tills in the section, and then incorporated these results into the age/depth model used to compute the ages of older units as we proceeded downward. When surficial loess was present, we assigned it an age of 0.1 $\pm$ 0.05 Ma. We took the surface erosion rate to be 10 $\pm$ 5 m Ma$^{-1}$ always. These assumptions are described and justified in detail in *S5*.

An important aspect of the present work is that we calculated all burial ages using a common set of isotope ratio standardizations, production rates, and decay constants, including $^{10}$Be and $^{26}$Al production rates by muons from *(S6)* and *(S7)*, $^{10}$Be and $^{26}$Al production rates by spallation from the global calibration data set and 'St' scaling scheme of *(S8)* (restandardized to the Be isotope ratio standards of *(S3)*), the $^{26}$Al half-life from *(S2)* (0.705 $\pm$ 0.017 Ma), and the $^{10}$Be half-life of *(S9)* and *(S10)* (1.387 $\pm$ 0.012 Ma) . For this reason, some burial ages for published data reported here differ from the originally published ages.

Uncertainties in burial ages include i) $^{26}$Al and $^{10}$Be measurement uncertainties, ii) site-specific uncertainties in the thicknesses, densities, ages, and estimated erosion rates of overburden units, iii) uncertainties in nuclide production rates by both spallation and muons, and iv) uncertainties in the $^{26}$Al and $^{10}$Be decay constants. Uncertainties are calculated by linearization, numerical partial differentiation, and adding in quadrature. *(S5)* and *(S11)* discuss the importance of various sources of uncertainty at length. For the all except one of the sites discussed in this work, the tills immediately overlying the paleosols we sampled are relatively thick ($>$ 1000 g cm$^{-2}$). In this situation, total uncertainties in the age are dominated by i) measurement uncertainties, and ii) uncertainties in the decay constants. In this situation, uncertainties in production rates and the burial history of the samples make a negligible contribution. At a single site (site 11 in Table 1, the intra-Alburnett paleosol at Conklin Quarry), the till overlying the samples was thinner (600 g cm$^{-2}$) and uncertainties in the burial history of the samples make a significant contribution to the total uncertainty in the burial age.

Figure S1 shows graphical solutions for burial ages at sites where we used the simple burial dating method; Figure S2 shows burial isochrons for sites where we used the isochron method.

*Adjustment to age model for DSDP 552a.* The timescale for DSDP Site 552A reported by Shackleton et al. *(S12)* was derived by linear interpolation between magnetostratigraphic boundaries with assigned ages of 1.66, 2.47, 2.92, and 3.40 Ma. The ages of these boundaries have since been revised to 1.78, 2.61, 3.05, and 3.59 Ma, respectively *(S13)*. Thus, we have piecewise-linearly adjusted the timescale of this core to reflect these new ages.

*References.*

S1. J. Stone *et al.*, *Methods and procedures, UW Cosmogenic Nuclide Lab.* (Available online: http://depts.washington.edu/cosmolab/chem.html)

S2. K. Nishiizumi, *Nucl. Instr. Methods* **B223-224**, 388-392 (2004).

S3. K. Nishiizumi *et al.*, *Nucl. Instr. Methods* **B258**, 403-413 (2007).

S4. G. Balco, C.W. Rovey II, J.O. Stone, *Science* **307**, 222 (2005)

S5. G. Balco, C.W. Rovey II, *Am. J. Sci.* **308**, 1083-1114 (2008).

S6. B. Heisinger *et al.*, *Earth Planet. Sci. Lett.* **200**, 345 (2002).

S7. B. Heisinger *et al.*, *Earth Planet. Sci. Lett.* **200**, 357 (2002).

S8. G. Balco *et al.*, *Quat. Geochron.* **3**, 174-195 (2008).

S9. J. Chmeleff *et al. Geochim. Cosmochim. Acta* **73**, A221 (2009).

S10. G. Korschinek *et al. Geochim. Cosmochim. Acta* **73**, A685 (2009)

S11. G. Balco, J.O. Stone, J. Mason, *Earth. Planet. Sci. Lett.* **232**, 179-191 (2005)

S12. N.J. Shackleton *et al.*, *Nature* **307**, 620 (1984).

S13. L. Lisiecki, M. Raymo, *Paleoceanography* **20**, PA1003 (2005).

S14. D. Granger, in *In-situ-produced cosmogenic nuclides and quantification of geological processes: Geological Society of America Special Paper 415*, L.L. Siame et al., Eds. (Geological Society of America, Boulder, CO, 2006), pp. 1-16.

S15. C. W. Rovey II, G. Balco, *Quaternary Research* (2009 in press). Reviewers can download this manuscript from:
http://depts.washington.edu/cosmolab/pubs/gb_pubs/pubs.html

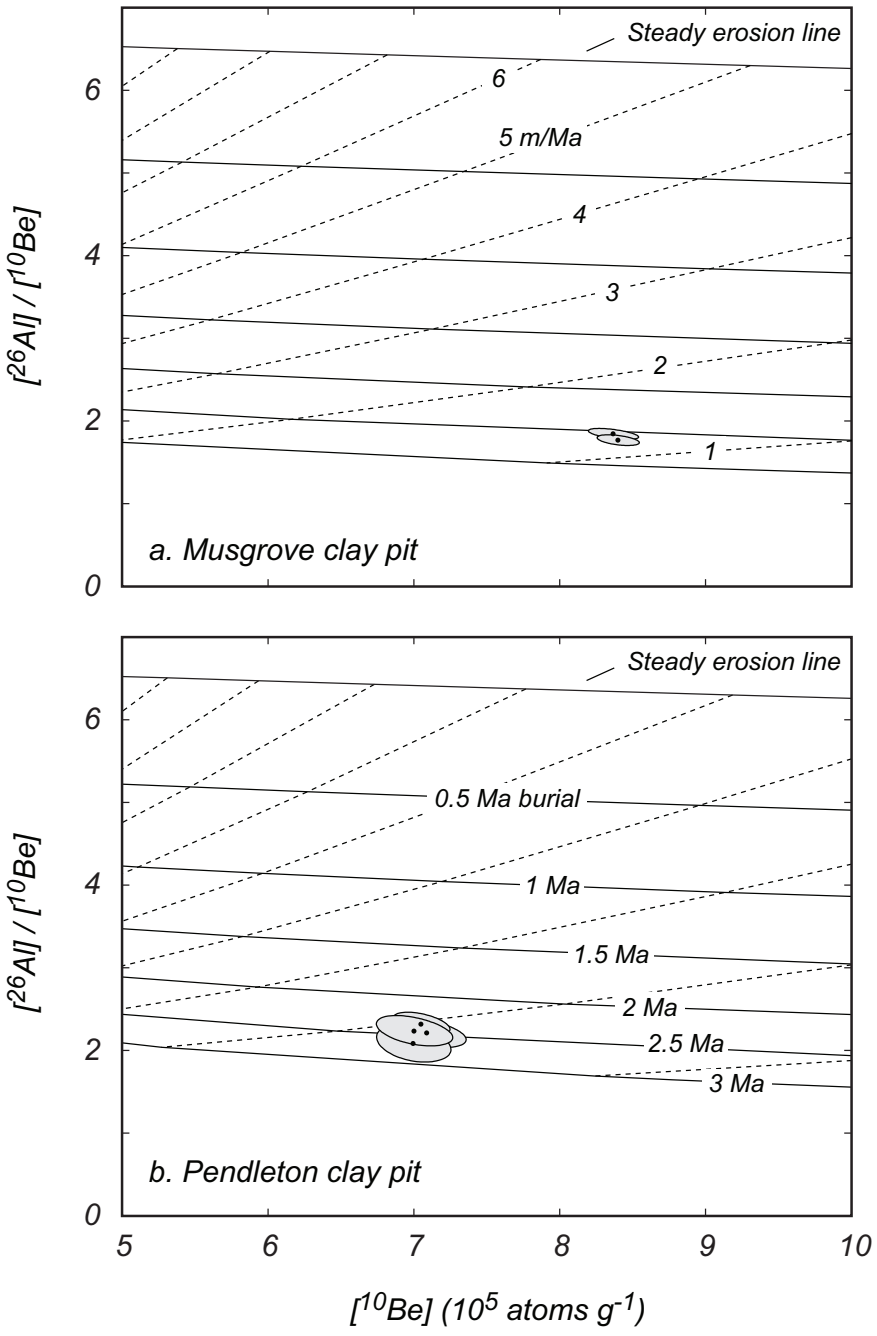


Figure S1a,b. $^{10}$Be - $^{26}$Al/$^{10}$Be diagram for samples from colluvium underlying the Atlanta Fm. at the Musgrove (a) and Pendleton (b) clay pits. The burial age of these samples is the age the Atlanta till was emplaced. See *(S14)* for a complete description of this diagram. The dashed lines are contours of surface erosion rate prior to burial and are labeled in the upper panel; the solid lines are contours of burial age and are labeled in the lower panel. In each diagram, the contours of burial age are drawn for the present depth of the samples. The gray ellipses are 68% confidence intervals reflecting measurement uncertainty.

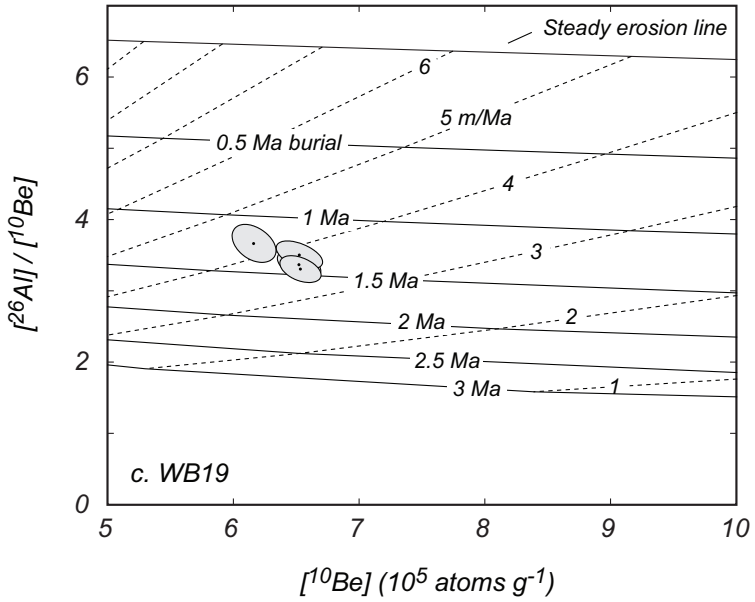


Figure S1c. $^{10}$Be - $^{26}$Al/$^{10}$Be diagram for samples from bedrock residuum underlying the Moberly Formation till in the WB19 borehole. The burial age of these samples is the age the Moberly Formation Formation till was emplaced. The diagram is constructed as described in the caption to Figure S1a.

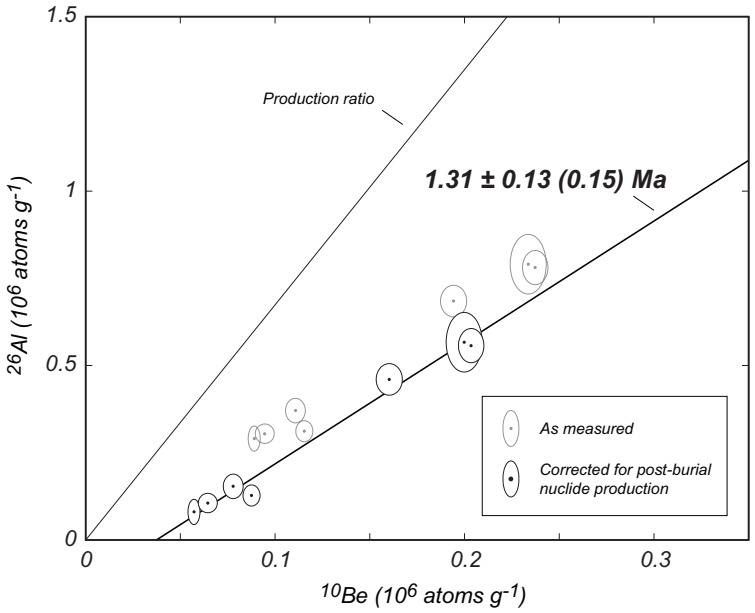


Figure S2a. $^{26}$Al - $^{10}$Be isochron for Atlanta Formation paleosol at the Musgrove clay pit. The burial age of these samples is the age of the overlying Moberly Formation till. In this and subsequent figures, the light gray ellipses are 68% confidence regions on measured $^{26}$Al and $^{10}$Be concentrations. The black ellipses reflect correction of the measured data for nuclide production after burial, as described in *(S5)*. The dark line is the isochron fit to the corrected data. The light line has a slope given by the $^{26}$Al/$^{10}$Be production ratio for comparison.

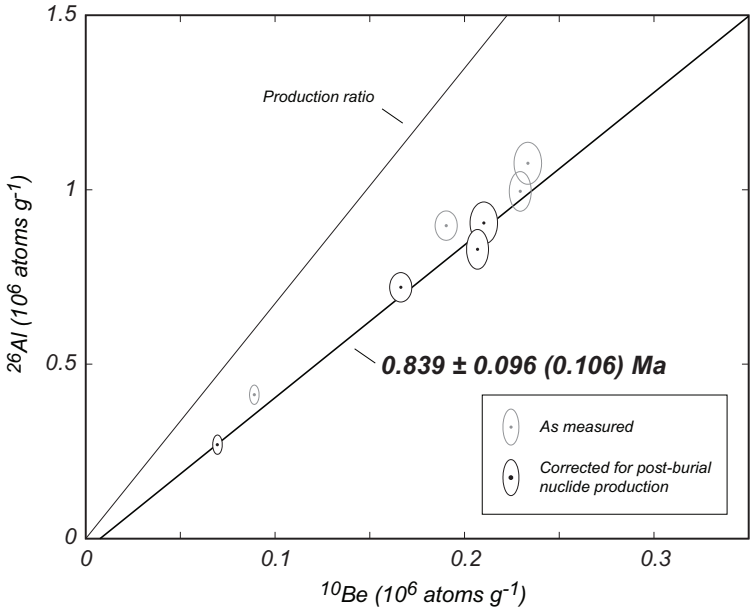


Figure S2b. $^{26}$Al - $^{10}$Be isochron for Moberly Formation paleosol in borehole FU02. The burial age of these samples is the age of the overlying Fulton till.

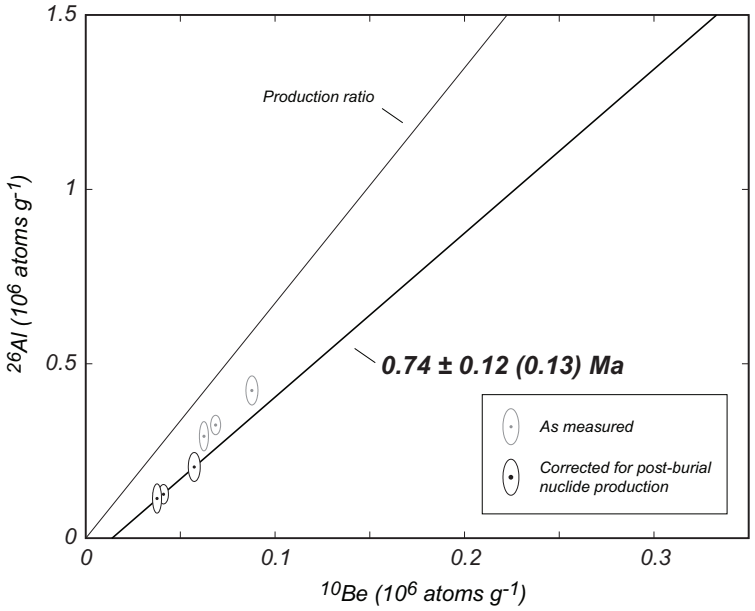


Figure S2c. $^{26}$Al - $^{10}$Be isochron for Moberly Formation paleosol in borehole NF06. The burial age of these samples is the age of the overlying Fulton till.

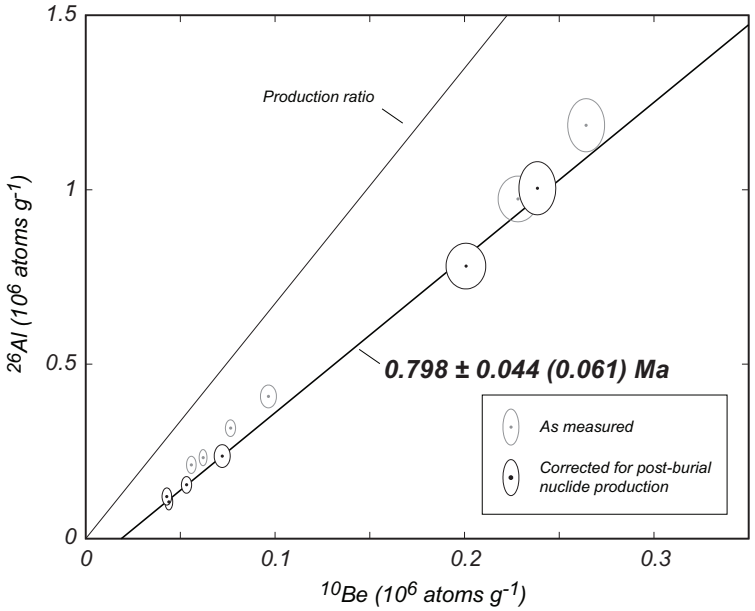


Figure S2d. $^{26}$Al - $^{10}$Be isochron for Moberly Formation paleosol in borehole WL3. The burial age of these samples is the age of the overlying Fulton till.

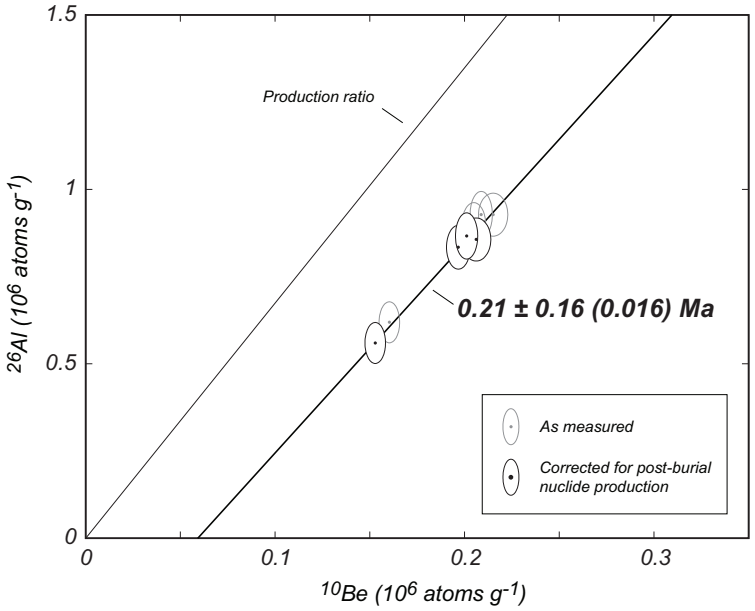


Figure S2e. $^{26}$Al - $^{10}$Be isochron for Fulton paleosol in borehole PF2. The burial age of these samples is the age of the overlying Columbia till.

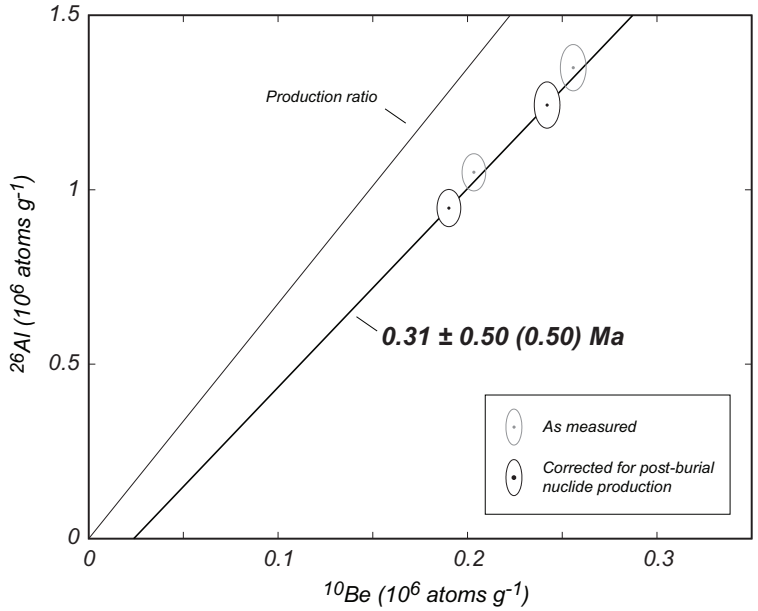


Figure S2f. $^{26}$Al - $^{10}$Be isochron for Fulton paleosol in borehole SMS92A. The burial age of these samples is the age of the overlying Columbia till.

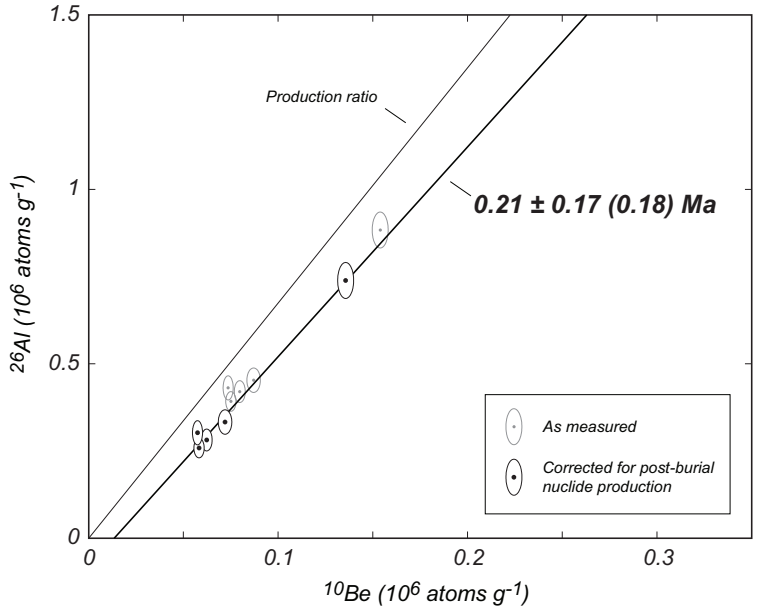


Figure S2g. $^{26}$Al - $^{10}$Be isochron for Columbia paleosol at the Sieger pit. The burial age of these samples is the age of the overlying Macon till.

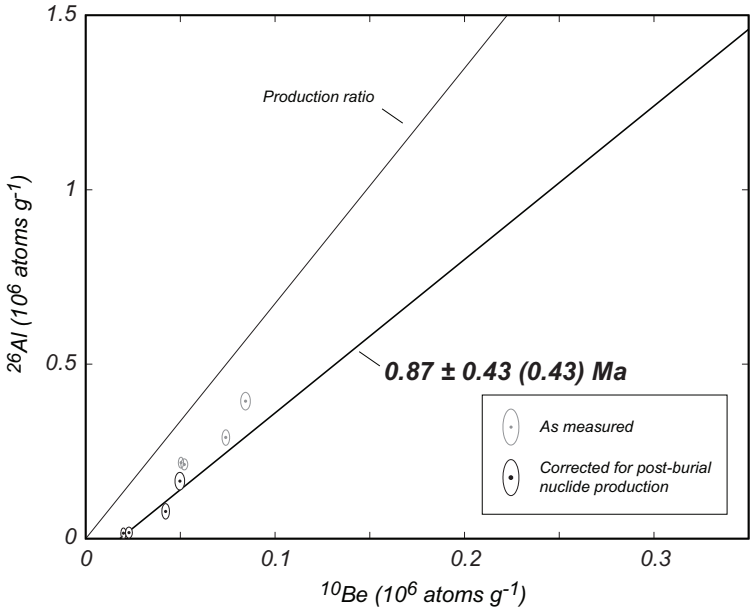


Figure S2h. $^{26}$Al - $^{10}$Be isochron for paleosol within the Alburnett Formation till at Conklin Quarry. The burial age of these samples is the age of the overlying portion of the Alburnett Fm. till.

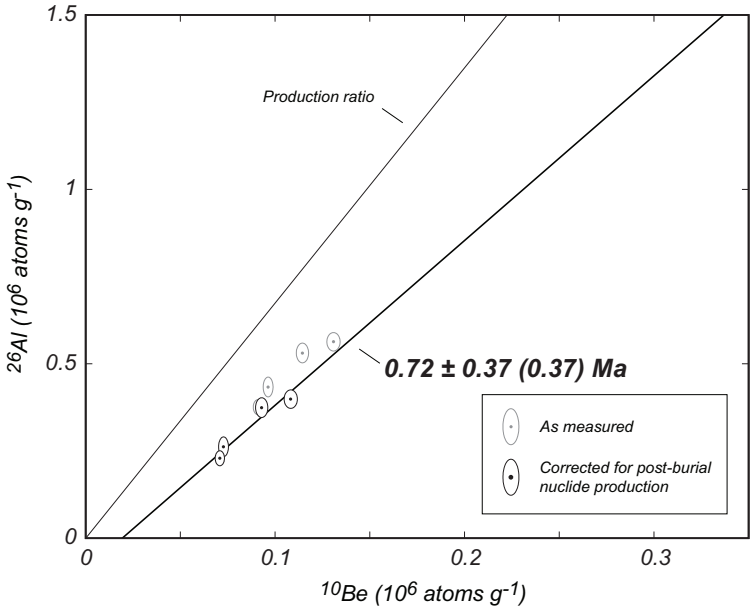


Figure S2i. $^{26}$Al - $^{10}$Be isochron for paleosol atop the Alburnett Formation till at Conklin Quarry. The burial age of these samples is the age of the overlying Winthrop till.